Semiclassical Interpretation of the Mass Asymmetry in Nuclear Fission

M. Brack,[1] S. M. Reimann,[2] and M. Sieber[3]
[1]*Institut für Theoretische Physik, Universität Regensburg, D-93040 Regensburg, Germany*
[2]*Niels Bohr Institutet, Blegdamsvej 17, DK-2100 Copenhagen Ø, Denmark*
[3]*Abteilung Theoretische Physik, Universität Ulm, D-89069 Ulm, Germany*
(Received 25 April 1997)

We give a semiclassical interpretation of the mass asymmetry in the fission of heavy nuclei. Using only a few classical periodic orbits and a cavity model for the nuclear mean field, we reproduce the onset of left-right asymmetric shapes at the fission isomer minimum and the correct topology of the deformation energy surface of ^{240}Pu in the region of the outer fission barrier. [S0031-9007(97)03997-5]

PACS numbers: 24.75.+i, 03.65.Sq, 21.10.Dr, 47.20.Ky

One characteristic feature of the fission of many actinide nuclei is the asymmetric mass distribution of the fission fragments. The liquid drop model [1], although capable of describing many aspects of the fission process qualitatively, cannot explain this mass asymmetry in heavy nuclei where the fissility parameter x is close to unity [2]: the balance between the attractive surface tension and the repulsive Coulomb force favors left-right symmetric shapes and thus also the symmetric fission. An explanation for the observed asymmetry, which sets in long before the nucleus breaks up (see below), became possible with Strutinsky's shell-correction method [3] which includes the quantal shell effects stemming from the discrete spectra of the nucleons in their mean fields. The total binding energy of a nucleus with N neutrons and Z protons is written as

$$E_{\rm tot}(N,Z;{\rm def}) = E_{\rm LDM}(N,Z;{\rm def}) + \delta E_n(N;{\rm def}) + \delta E_p(Z;{\rm def}) . \quad (1)$$

Here $E_{\rm LDM}$ is the liquid drop model (LDM) energy; δE_n and δE_p are the shell-correction energies of the neutrons and protons, respectively, which are obtained in terms of the single-particle energies of realistic shell-model potentials. All ingredients depend on the shape of the nucleus, which is described by some suitable deformation parameters, summarized in (1) by "def." The shell-correction approach was very successful in reproducing experimental nuclear binding energies and fission barriers [4–6] at times where self-consistent microscopical calculations of Hartree-Fock type were not yet available [7].

Figure 1 shows a schematic fission barrier of a typical actinide nucleus, taken along the adiabatic path through the multidimensional deformation space. The heavy dashed line is the LDM deformation energy which leads to a spherical ground state and to symmetric fission. The solid line is the total energy (1) including the shell corrections δE_n and δE_p. These lead to a deformed ground-state minimum and a higher-lying minimum, the fission isomer [8]. The shapes used hereby have axial symmetry and left-right symmetry. When the latter is relaxed, the energy is found [9,10] to be lowered along the way over the outer barrier, starting at the fission isomer. (The axial symmetry is preserved in the whole region beyond the inner barrier [11].) The energy gain due to left-right asymmetry persists all the way down to the scission point where the nucleus breaks into two fragments of unequal size. It is important to note that the onset of the mass asymmetry occurs already at an early stage of the fission process, long before the nucleus breaks up. It is a pure quantum effect which only comes about if the shell corrections are included in the total energy. Dynamical calculations [12] are needed to predict the detailed fragment mass distributions, but the most probable mass ratio is roughly that of the nascent fragments found statically at the asymmetric outer barrier [4]. The microscopic origin of the static instability against left-right asymmetry has been investigated by Gustafsson, Möller, and Nilsson [13]. They found that only two specific types of single-particle states with large angular momenta along the symmetry axis are strongly sensitive to the left-right asymmetry: one of them has the maxima of its wave functions along the central waistline of the nucleus (see the upper right in Fig. 1), whereas the other has maxima along the circumferences of two equatorial planes at some distance of the center (with opposite phases on either side; see the middle right in Fig. 1). The coupling of these states through the left-right asymmetric components of the mean

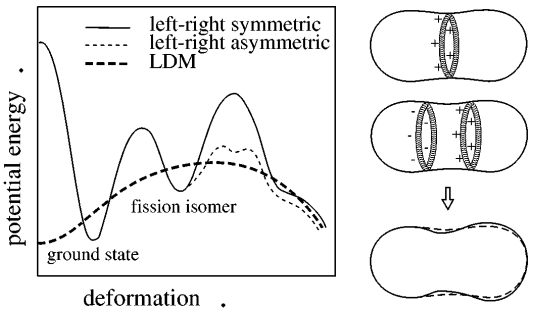

FIG. 1. Left: Schematic fission barrier of a typical actinide nucleus. Right: Schematic probability amplitudes of leading single-particle wave functions responsible for the onset of mass asymmetry (after Ref. [13]).

field leads to a decrease of one set of eigenenergies below the Fermi energy, and thus to a reduction of the total energy, when the asymmetry is switched on.

In the following we give a very simple and transparent semiclassical interpretation of this static quantum effect. We employ the periodic orbit theory (POT) [14,15] which expresses the oscillating part of the level density of a quantum system semiclassically through the so-called "trace formula,"

$$\delta g(E) \simeq \mathrm{Re} \sum_{\mathrm{PO}} \mathcal{A}_{\mathrm{PO}}(E) e^{i[(1/\hbar)S_{\mathrm{PO}}(E) - \sigma_{\mathrm{PO}}(\pi/2)]}. \quad (2)$$

The sum is taken over all periodic orbits, labeled "PO," of the corresponding classical system. S_{PO} are the classical actions along the periodic orbits, and σ_{PO} are phases related to the number of conjugate points along the orbits. The amplitude $\mathcal{A}_{\mathrm{PO}}$ of each orbit depends on its period, its stability, and its degeneracy. Together with the smooth part $\tilde{g}(E)$ which can be obtained in the (extended) Thomas-Fermi model, it approximates the exact quantum-mechanical level density, $\tilde{g}(E) + \delta g(E) = g(E) = \sum_i \delta(E - E_i)$, where E_i are the eigenenergies of the system and the sum runs over all quantum states i. (See Ref. [16] for an introduction to the POT and detailed explanations of all the above ingredients.) Gutzwiller's trace formula [14] has been applied for the semiclassical quantization of chaotic systems [17]. A different use of the POT [16,18] is to obtain a coarse-grained level density by keeping only the shortest orbits with the largest amplitudes in the trace formula (2). This allows one to relate the gross-shell structure of interacting fermion systems in the mean-field approximation to a few classical orbits. Using Eq. (2), the semiclassical expression for the energy shell correction δE becomes

$$\delta E \simeq \mathrm{Re} \sum_{\mathrm{PO}} \mathcal{A}_{\mathrm{PO}}(E_F) \left(\frac{\hbar}{T_{\mathrm{PO}}} \right)^2 e^{i[(1/\hbar)S_{\mathrm{PO}}(E_F) - \sigma_{\mathrm{PO}}(\pi/2)]}. \quad (3)$$

Here E_F is the Fermi energy and $T_{\mathrm{PO}} = dS_{\mathrm{PO}}/dE|_{E_F}$ the period of the orbit labeled PO. Pioneering work has been done in this direction by Strutinsky *et al.* [18], who generalized the Gutzwiller theory to systems with continuous symmetries and used it to give a semiclassical explanation of the systematics of nuclear ground-state deformations. Another beautiful example is the beating pattern of the coarse-grained level density in a spherical cavity, which was related by Balian and Bloch [15] to the interference of the triangular and square periodic orbits, and later predicted [19] and observed [20] in metal clusters in the form of the so-called supershells. Arita and Matsuyanagi [21] have studied the effect of left-right asymmetric deformations of octupole type on the supershell structure in harmonic-oscillator potentials and discussed them in terms of periodic orbits.

For our semiclassical investigation, we replace the nuclear mean field by a cavity with reflecting walls and consider only one kind of particles. This should yield the main physical effects, since the neutron contribution δE_n contains the strongest shell effects, as seen, e.g., in Fig. VIII-4 of Ref. [4]. We employ the parametrization (c, h, α) of this reference to define the boundary of the cavity in cylindrical coordinates (ρ, z, ϕ) (with z as the symmetry axis) through a shape function $\rho = \rho(z; c, h, \alpha)$. c is the length of the semiaxis along z in units of the radius R_0 of the spherical cavity given by $c = 1$, $h = \alpha = 0$. h is a "neck parameter" regulating the formation of a neck leading to the scission of the nucleus into two fragments. $\alpha \neq 0$ yields left-right asymmetric shapes. The volume of the cavity is kept constant. (See Ref. [4] for details of this parametrization, and especially Figs. VII-1 and VIII-5 for the most important shapes occurring in fission.) The parameters (c, h) are chosen such that the one-dimensional curve $h = \alpha = 0$ along c follows the adiabatic fission barrier of the LDM (shown schematically in Fig. 1). Even including the shell effects, $h = 0$ gives a reasonable picture of the double-humped fission barrier.

We now have to determine the shortest periodic orbits of this system to calculate the gross-shell structure in δE. At large deformations (here $c \gtrsim 1.4$), these are the orbits lying in equatorial planes perpendicular to the symmetry axis [22]. The positions z_i of these planes along the z axis are given by the condition that the shape function be stationary: $d\rho(z; c, h, \alpha)/dz|_{z_i} = 0$. The periodic orbits have the form of regular polygons and are characterized by (p, t), where p is the number of reflections at the boundary and t the number of windings around the symmetry axis ($p \geq 2$, $t \leq p/2$). The contribution of such orbits to Eq. (2) has been derived by Balian and Bloch [15]; we refer to their paper for the explicit form of the amplitudes $\mathcal{A}_{pt}$ and phases σ_{pt}. The lengths of the orbits are $L_{pt}^{(i)} = 2pR_i \sin(\pi t/p)$, where $R_i = \rho(z_i; c, h, \alpha)$, and their actions are $S_{pt}^{(i)}(E_F) = \hbar k_F L_{pt}^{(i)}$ in terms of the Fermi wave number $k_F = \sqrt{2mE_F}/\hbar$.

The range of validity of Eqs. (2) and (3) is, however, limited. They are correct only as long as the orbits are well separated from neighboring periodic orbits, in particular, as long as the orbits are not close to a bifurcation. At a bifurcation the amplitudes $\mathcal{A}_{pt}$ diverge and the trace formula has to be modified. Generally, bifurcations exist in different forms, but for the situation studied here we need consider only one type of bifurcation. It occurs when the positions z_i of several equatorial planes coincide. In the (c, h, α) parametrization, there are at most three such planes. One plane always exists; the other two arise at the points (c_0, h_0, α_0) where the neck formation starts. In the symmetric case ($\alpha = 0$), one plane is always located at $z_0 = 0$ and, beyond the bifurcation point, the other two are located symmetrically at $\pm z_1$ (with $z_1 > 0$) and contain identical periodic orbits.

Near a bifurcation point, all neighboring orbits of type (p, t) from the different planes give a joint contribution to the level density which is given [15] by an integral of the form

$$\delta E_{pt} = \mathrm{Re} \int_{-c}^{+c} dz\, f_{pt}(z) \exp\{ik_F L_{pt}(z)\}, \qquad (4)$$

where $f_{pt}(z)$ is a slowly varying analytic function of z. Since the plane positions z_i of the periodic orbits are determined by the stationary points of the length function $L_{pt}(z) = 2p \sin(\pi t/p)\rho(z; c, h, \alpha)$, a stationary phase evaluation of (4) leads back to separate contributions to Eq. (3) for each plane, with the amplitudes and phases given in [15]. In order to obtain an approximation to (4) that is valid at the bifurcation as well as far from it, we employ a uniform approximation appropriate for the case of three nearly coincident stationary points in a one-dimensional oscillatory integral [23]. It is expressed in terms of Pearcey's integral and its derivatives,

$$\delta E_{pt} = \mathrm{Re}\,\{[u_4 P(u_1, u_2) + u_5 P_x(u_1, u_2) + u_6 P_y(u_1, u_2)] e^{iu_3}\}, \qquad (5)$$

where Pearcey's integral is defined by

$$P(x, y) = \int_{-\infty}^{\infty} dz\, \exp[\, i(z^4 + xz^2 + yz)], \qquad (6)$$

and $P_x(x, y)$, $P_y(x, y)$ denotes its derivative with respect to the first and second argument, respectively. The constants $u_1 \ldots u_6$ are determined by the semiclassical amplitudes, actions, and phases of the periodic orbits. If the orbits are well separated, Eq. (5) reduces to contributions to the standard trace formula (3).

In the symmetric case ($\alpha = 0$), the result (5) can be simplified and yields a formula which is analogous to that for a generic pitchfork bifurcation [24],

$$\delta E_{pt} = \mathrm{Re}\sqrt{\frac{\pi k_F |\Delta L_{pt}|}{2}} \left\{ \left(\frac{\hbar^2 \mathcal{A}_{pt}^{(1)}}{[T_{pt}^{(1)}]^2} + \frac{\hbar^2 \mathcal{A}_{pt}^{(0)}}{\sqrt{2}[T_{pt}^{(0)}]^2} \right) [\nu J_{1/4}(k_F|\Delta L_{pt}|)\, e^{i\pi/8} + J_{-1/4}(k_F|\Delta L_{pt}|)\, e^{-i\pi/8}] \right.$$
$$\left. + \left(\frac{\hbar^2 \mathcal{A}_{pt}^{(1)}}{[T_{pt}^{(1)}]^2} - \frac{\hbar^2 \mathcal{A}_{pt}^{(0)}}{\sqrt{2}[T_{pt}^{(0)}]^2} \right) [J_{3/4}(k_F|\Delta L_{pt}|)\, e^{i3\pi/8} + \nu J_{-3/4}(k_F|\Delta L_{pt}|)\, e^{-i3\pi/8}] \right\}$$
$$\times\, e^{i(k_F \bar{L}_{pt} - 3p\pi/2)}. \qquad (7)$$

Here $\bar{L}_{pt} = [L_{pt}^{(1)} + L_{pt}^{(0)}]/2$ and $\Delta L_{pt} = [L_{pt}^{(1)} - L_{pt}^{(0)}]/2$ in terms of the lengths $L_{pt}^{(0)}$, $L_{pt}^{(1)}$ of the orbits pt situated at $z = z_0$ and $z = \pm z_1$, respectively. ν equals -1 before the bifurcation (i.e., for only one orbit plane) and $+1$ after the bifurcation (for three orbit planes). In the general case $\alpha \neq 0$, however, the entire Pearcey integral and its derivatives have to be used and evaluated numerically.

In the right-hand panels of Fig. 2 we show contour plots of the semiclassical shell-correction energy δE in the (c, α) plane for two values of the neck parameter. The energy unit is $E_0 = \hbar^2/2mR_0^2$. The Fermi wave number $k_F = 12.1/R_0$ was chosen such that δE has a minimum at the deformation $c = 1.42$, $h = \alpha = 0$ of the fission isomer. On the left of Fig. 2 we have reproduced the neutron shell-correction energy δE_n of the nucleus ^{240}Pu, obtained in Ref. [4] with a realistic Woods-Saxon type shell-model potential. We see that the semiclassical result correctly reproduces the topology of the deformation energy in the (c, α) plane for both values of h, in particular, the onset of the mass asymmetry at the fission isomer. It should be noted that we have only included orbits with winding number one ($t = 1$) and with up to $p_{\max} = 10$ reflections. The results for δE remain the same within a few percent when only orbits with $p = 2$ and 3 (i.e., only diameter and triangle orbits) are included. In the quantum results [4] for δE, pairing correlations are included. These lead to a suppression of the longer periodic orbits. Furthermore, the semiclassical amplitudes in (3) are suppressed by the inverse squared periods T_{PO}. As net result, equatorial orbits with winding numbers $t > 1$ and other longer orbits will not alter the results within the present resolution of the shell effects in δE. A detailed comparison with quantum-mechanical calculations in the same cavity model, which confirm the excellent quality of our semiclassical approach, will be published shortly [25].

The loci of the bifurcation points (c_0, α_0) are indicated in Fig. 2 by the black heavy dashed lines (hardly visible for $h = -0.075$ in the upper right corner). This shows that the essential feature, namely, the energy gain due to the asymmetric deformations, is brought about by only two classical orbits: the diameter and the triangle in the central equatorial plane. The white dashed lines give the loci of constant actions of the periodic orbits at z_0, fixing their value at $\alpha = 0$. (Note that the actions of all orbits in a given equatorial plane have the same deformation dependence.) We see that the valley that leads from

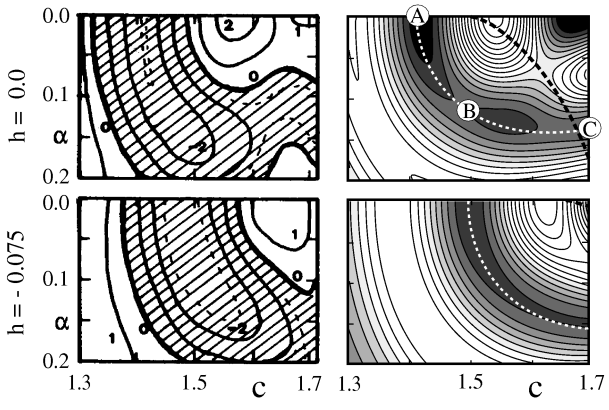

FIG. 2. Contour plots of deformation energy versus elongation c and asymmetry α for two values of the neck parameter: $h = 0$ (above) and $h = -0.075$ (below). Left: Quantum-mechanical neutron shell correction δE_n of ^{240}Pu [4]. Right: Semiclassical shell-correction energy δE, (3) and (5). White dashed lines are the loci of constant action of the central equatorial orbits; black dashed lines the loci of the bifurcations.

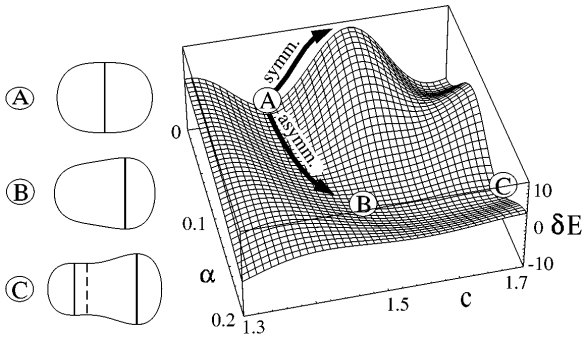

FIG. 3. Right: $\delta E(c, \alpha)$ as in Fig. 2 (for $h = 0$) in a 3D plot. Arrows "symmetric" and "asymmetric" show two alternative fission paths. Left: Shapes along the asymmetric fission path. The planes of the leading periodic orbits are shown by vertical lines (solid for stable and dashed for unstable orbits).

the isomer minimum over the outer fission barrier in the energetically most favorable way is following exactly the path of constant action of the leading classical orbits; this path is practically identical with that obtained in the quantum-mechanical shell-correction calculations.

In Fig. 3, we show the same results as in the upper right part of Fig. 2, but in a perspective view of a three-dimensional energy surface. On the left, the shapes of the cavity are given corresponding to the points A at the isomer minimum and the points B and C along the asymmetric fission barrier (see also the corresponding points in Fig. 2). Note that C lies beyond the bifurcation point and thus contains three planes of periodic orbits.

In summary, we have shown how a specific quantum effect, causing a drastic rearrangement of the shape of a complex many body system, can be described semiclassically by the constancy of the actions of the shortest periodic orbits. With this, we have for the first time given a semiclassical interpretation of the mechanism leading to the asymmetry of nuclear fission. We also point at the close correspondence of the equatorial planes of the leading orbits (cf. Fig. 3, left) with the locations of the wave function maxima (cf. Fig. 1, right) of the relevant quantum states. Whether this constitutes an analog of the so-called "scars," which are of strong current interest in connection with chaotic systems (see, e.g., Ref. [26]), will be investigated in further studies. Note that the classical dynamics of the present system is also predominantly chaotic on subspaces of small angular momenta L_z [21]. Still, the regular regions in phase space, connected to the stable periodic orbits with axial degeneracy, are strong enough to cause this important shell effect.

This work was supported in part by the Deutsche Forschungsgemeinschaft under Contracts No. Ste 241/6-1 and No. Ste 241/7-2, by Studienstiftung des Deutschen Volkes, and by BASF-AG.

[1] N. Bohr and J. A. Wheeler, Phys. Rev. **56**, 426 (1939).

[2] $x = E_c/2E_s$, where E_c and E_s are the Coulomb and surface energies, respectively, of the charged spherical liquid drop. When $x \geq 1$, the drop is unstable against fission. For further details see, e.g., L. Wilets, *Theories of Nuclear Fission* (Clarendon Press, Oxford, 1964).

[3] V. M. Strutinsky, Nucl. Phys. **A122**, 1 (1968), and references therein.

[4] M. Brack, J. Damgård, A. S. Jensen, H. C. Pauli, V. M. Strutinsky, and C. Y. Wong, Rev. Mod. Phys. **44**, 320 (1972).

[5] S. G. Nilsson, C. F. Tsang, A. Sobiczewski, Z. Szymański, S. Wycech, C. Gustafsson, I.-L. Lamm, P. Möller, and B. Nilsson, Nucl. Phys. **A131**, 1 (1969).

[6] M. Bolsterli, E. O. Fiset, J. R. Nix, and J. L. Norton, Phys. Rev. C **5**, 1050 (1972); J. R. Nix, Annu. Rev. Nucl. Sci. **22**, 65 (1972).

[7] See Refs. [3,4] for the foundation of the shell-correction method on the Hartree-Fock theory, and M. Brack and P. Quentin, Nucl. Phys. **A361**, 35 (1981), for numerical tests employing realistic nucleon-nucleon interactions.

[8] For an extended review on the physics of the "double-humped fission barrier," see S. Bjørnholm and J. E. Lynn, Rev. Mod. Phys. **52**, 725 (1980).

[9] P. Möller and S. G. Nilsson, Phys. Lett. **31B**, 283 (1970).

[10] H. C. Pauli, T. Ledergerber, and M. Brack, Phys. Lett. **34B**, 264 (1971).

[11] See, M. Brack, in *Physics and Chemistry of Fission 1979* (IAEA, Vienna, 1980), Vol. I, p. 227, for a short review on fission barrier calculations and the role of symmetries.

[12] See, e.g., J. Maruhn, W. Greiner, P. Lichtner, and D. Drechsel, in *Physics and Chemistry of Fission 1973* (IAEA, Vienna, 1974), Vol. I, p. 569.

[13] C. Gustafsson, P. Möller, and S. G. Nilsson, Phys. Lett. **34B**, 349 (1971).

[14] M. C. Gutzwiller, J. Math. Phys. (N.Y.) **12**, 343 (1971).

[15] R. Balian and C. Bloch, Ann. Phys. (N.Y.) **69**, 76 (1972).

[16] M. Brack and R. K. Bhaduri, *Semiclassical Physics* (Addison and Wesley, Reading, 1997).

[17] See, e.g., special issue *Chaos Focus Issue on Periodic Orbit Theory*, edited by P. Cvitanović [Chaos **2**, 1–158 (1992)].

[18] V. M. Strutinsky and A. G. Magner, Sov. J. Part. Nucl. **7**, 138 (1976); V. M. Strutinsky, A. G. Magner, S. R. Ofengenden, and T. Døssing, Z. Phys. A **283**, 269 (1977).

[19] H. Nishioka, K. Hansen, and B. R. Mottelson, Phys. Rev. B **42**, 9377 (1990).

[20] J. Pedersen, S. Bjørnholm, J. Borggreen, K. Hansen, T. P. Martin, and H. D. Rasmussen, Nature (London) **353**, 733 (1991).

[21] K. Arita and K. Matsuyanagi, Nucl. Phys. **A592**, 9 (1995). For very recent similar studies in octupole-deformed cavities, see A. Sugita, K. Arita, and K. Matsuyanagi, Kyoto University Report No. KUNS1431, 1997.

[22] H. Frisk, Nucl. Phys. **A511**, 309 (1990).

[23] J. N. L. Connor, Mol. Phys. **26**, 1217 (1973).

[24] H. Schomerus and M. Sieber, J. Phys. A **30**, 4537 (1997).

[25] M. Brack, P. Meier, S. R. Reimann, and M. Sieber (to be published).

[26] E. J. Heller, in *Chaos and Quantum Physics*, Proceedings of the Les Houches Summer School, Lectures LII, edited by M.-J. Giannoni, A. Voros, and J. Zinn-Justin (North-Holland, Amsterdam, 1991), p. 547.